UC Riverside

UC Riverside Previously Published Works

Title

A pH-Based Pedotransfer Function for Scaling Saturated Hydraulic Conductivity Reduction: Improved Estimation of Hydraulic Dynamics in HYDRUS

Permalink

https://escholarship.org/uc/item/7mt7t8jd

Journal

VADOSE ZONE JOURNAL, 18(1)

Authors

Ali, Aram
Biggs, Andrew JW
Simunek, Jirka
et al.

Publication Date

2019

DOI

10.2136/vzj.2019.07.0072

Peer reviewed

eScholarship.org Powered by the California Digital Library
University of California

Published November 22, 2019

Original Research

Core Ideas

- Soil-specific pedotransfer functions can be incorporated into the HYDRUS model.
- Electrolyte concentration reduces the adverse effect of pH and Na on soil structural stability.
- Clay content is important in governing soil hydraulic reduction dynamics due to pH.

A pH-Based Pedotransfer Function for Scaling Saturated Hydraulic Conductivity Reduction: Improved Estimation of Hydraulic Dynamics in HYDRUS

Aram Ali,* Andrew J.W. Biggs, Jirka Šimůnek, and John McL. Bennett

Hydraulic conductivity is a key soil property governing agricultural production and is thus an important parameter in hydrologic modeling. The pH scaling factor for saturated hydraulic conductivity (K_s) reduction in the HYDRUS model was reviewed and evaluated for its ability to simulate K_s reduction. A limitation of the model is the generalization of K_s reduction at various levels of electrolyte concentration for different soil types, i.e., it is not soil specific. In this study, a new generalized linear regression model was developed to estimate K_s reduction for a larger set of Australian soils compared with three American soils. A nonlinear pedotransfer function was also produced, using the Levenberg–Marquardt optimization algorithm, by considering the pH and electrolyte concentration of the applied solution as well as the soil clay content. This approach improved the estimation of the pH scaling factor relating to K_s reduction for individual soils. The functions were based on K_s reduction in nine contrasting Australian soils using two sets of treatment solutions with Na adsorption ratios of 20 and 40; total electrolyte concentrations of 8, 15, 25, 50, 100, 250, and 500 $mmol_c\ L^{-1}$; and pH values of 6, 7, 8, and 9. A comparison of the experimental data and model outputs indicates that the models performed objectively well and successfully described the K_s reduction due to the pH. Further, a nonlinear function provided greater accuracy than the generalized function for the individual soils of Australia and California. This indicates that the nonlinear model provides an improved estimation of the pH scaling factor for K_s reduction in specific soils in the HYDRUS model and should therefore be considered in future HYDRUS developments and applications.

Abbreviations: EC, electrolyte concentration; SAR, sodium adsorption ratio.

A. Ali, A.J.W. Biggs, J. Šimůnek, and J.McL. Bennett, Univ. of Southern Queensland, Centre for Sustainable Agricultural Systems, West St, Toowoomba, QLD 4350, Australia; A.J.W. Biggs, Dep. of Natural Resources, Mines and Energy, Tor St, Toowoomba, QLD 4350, Australia; J. Šimůnek, Dep. of Environmental Sciences, Univ. of California, Riverside, CA 92521. *Corresponding author (aram.ali@usq.edu.au).

Received 7 July 2019.
Accepted 28 Oct. 2019.

Citation: Ali, A., A.J.W Biggs, J. Šimůnek, and J.M. Bennett. 2019. A pH-based pedotransfer function for scaling saturated hydraulic conductivity reduction: Improved estimation of hydraulic dynamics in HYDRUS. Vadose Zone J. 18:190072. doi:10.2136/vzj2019.07.0072

© 2019 The Author(s). This is an open access article distributed under the CC BY-NC-ND license (http://creativecommons.org/licenses/by-nc-nd/4.0/).

Soil hydraulic conductivity is a critically important soil physical property used in determining water and solute transport, infiltration rate, groundwater recharge, and other agricultural and hydrological processes (Ben-Hur et al., 2009; Smith et al., 1995). Soil hydraulic conductivity is strongly dependent on soil structural status and stability and the geometry of pore spaces in the soil (Assouline and Narkis, 2011). The use of marginal quality irrigation water is likely to cause deterioration in the soil structure; a change in the ratio of solids, water, and air within the soil; and reduced hydraulic conductivity due to clay disaggregation and dispersion processes (Bennett et al., 2019; Quirk and Schofield, 1955; Rengasamy and Olsson, 1991). A reduction in hydraulic conductivity often occurs as a result of excess Na within the soil solution (measured as the sodium adsorption ratio, SAR), which can result in both intra- and inter-crystalline swelling, leading to clay dispersion (Dang et al., 2018b; Ezlit et al., 2013). The magnitude of the reduction in hydraulic conductivity depends on the electrolyte concentration (EC) in the soil solution (Quirk and Schofield, 1955; Shainberg and Letey, 1984). Furthermore, Suarez et al. (1984) showed that the pH of the solute percolating a soil, in combination with high SAR and low EC, was likely to lead to decreased hydraulic conductivity beyond the combined SAR and EC effect alone. The effects of pH, EC, and SAR of an applied solution on soil hydraulic conductivity have been broadly investigated, experimentally and mathematically, using

predictive models (Chorom et al., 1994; Ezlit et al., 2013; McNeal and Coleman, 1966; Suarez and Rubio, 2010).

Predictive models have become efficient tools to investigate water flow and solute movement in soils under irrigation. The performance of multiple simulations considering various equilibrium and kinetic nonequilibrium chemical reactions between major ions allows industry and research to quickly interrogate the dynamics of systems. However, the development of models for the prediction of soil structural degradation and hydraulic conductivity dynamics will only be as good as the functions and assumptions that underlie them. Saturated hydraulic conductivity reduction remains a challenging task due to the combined effects of sodicity, salinity, pH, and alkalinity within the context of the soil being an inherently heterogeneous and complex material that is non-rigid (Campbell and Paustian, 2015; Miller and White, 1998). Therefore, the effect of a given solution chemistry can lead to unique soil structural dynamics within soils of different origin (Bennett et al., 2019; Bennett and Warren, 2015; Menezes et al., 2014; Quirk and Schofield, 1955), soil clay content and mineral suite (Bell, 1996; Goldberg and Glaubig, 1987), soil organic matter (Oades, 1984), the pH of soil solution (Bolan et al., 1996; Suarez et al., 1984), and the ionicity of the soil aggregate system (Bennett et al., 2019; Marchuk and Rengasamy, 2012; Zhu et al., 2019). Moreover, the magnitudes and the interrelationship of these factors provide variable levels of resilience of soils to structural degradation for a given intervention. Therefore, soil hydraulic dynamics should not be expected to be simply predicted with a generalized model.

The HYDRUS model is perhaps the most widely utilized soil hydraulic model (Šimůnek et al., 2016). The empirical and semiempirical equations for the adverse effects of SAR, EC, and pH of solutions are described within the HYDRUS program manual (Šimůnek et al., 2013). McNeal (1968) used a semiempirical equation based on the experimental clay swelling function for montmorillonite clay treated with combined sodic and saline solutions to fit experimental curves related to the relative saturated hydraulic conductivity (K_s). The effect of solution pH on the K_s is derived from Suarez et al. (1984), whereby the change in K_s is characterized by a negative effect of pH on the soil hydraulic conductivity, independent of EC and SAR, which is explained by an additional scaling factor. Suarez et al. (1984) investigated the effects of pH on the K_s of three soils from California for a combination of solution SAR and EC concentrations; i.e., pH cannot be thought of as completely independent of the SAR and EC, as this is not physically possible. The results of the Suarez et al. (1984) study, using a narrow range of soils, have become the main dataset for the prediction of K_s reduction due to the pH of the applied solution. Furthermore, this dataset was subsequently used to produce a linear function (see Eq. [4] below) to simulate r_{Ks} reduction due to pH in the UNSATCHEM and HYDRUS mathematical models of Suarez and Šimůnek (1997) and Šimůnek and Suarez (1997).

The use of this reduction model is likely to provide less accurate prediction of K_s for different soils (Šimůnek and Suarez, 1997) but to some extent helps to identify the degree of K_s reduction due to the pH of applied solutions. Therefore, there is a global need to optimize and validate the model parameters for pH-induced K_s reduction within the HYDRUS model and more broadly for use as a pedotransfer function. However, the approaches to validate and calibrate the models vary depending on the complexity involved in parameterizing of the models. Šimůnek et al. (2012) indicated that model calibration and inverse parameter estimation can be performed using a relatively simple, gradient based, local optimization approach based on the Marquardt–Levenberg method, which is directly implemented into the HYDRUS codes; it is also important that the estimated model is both efficient and robust. This study reviewed the HYDRUS model for K_s reduction due to the pH of the applied solution and developed modifications to the current reduction model and its parameters. This was achieved by combining Levenberg–Marquardt nonlinear parameter optimization involving the EC and pH of the applied solution, as well as the soil clay content, to improve the accuracy of the modeled solute and water movement on a soil-specific basis.

Theoretical Background

Within HYDRUS, the reduction of the hydraulic conductivity K is calculated by multiplying a scaling factor r with the initial saturated hydraulic conductivity K_s and the relative hydraulic conductivity K_r. The scaling factor r is a function of the soil solution pH, SAR, and EC, and the relative hydraulic conductivity K_r is a function of the hydraulic pressure head:

$$K(h, p\mathrm{H}, \mathrm{SAR}, \mathrm{EC}) = r(\mathrm{pH}, \mathrm{SAR}, \mathrm{EC}) K_s K_r(h) \quad [1]$$

where K is the hydraulic conductivity (cm d^{-1}), h is the pressure head (cm), pH is the solution pH (–log[H^+]), SAR is the sodium adsorption ratio, EC is the total electrolyte concentration of the solution ($mmol_c\ L^{-1}$), and r is a scaling factor (a function of pH, SAR, and EC). Subsequently, the scaling parameter, r, is divided into two sub-factors:

$$r(\mathrm{pH}, \mathrm{SAR}, \mathrm{EC}) = r_1(\mathrm{SAR}, \mathrm{EC}) r_2(\mathrm{pH}) \quad [2]$$

where r_1 is a function of SAR and EC, providing the disaggregation (inter- and intra-crystalline swelling) and dispersion effects on the hydraulic conductivity, as described by Quirk and Schofield (1955), Dang et al. (2018b), and Bennett et al. (2019), while r_2 represents the effects of solution pH on the hydraulic conductivity (Suarez et al., 1984). The assumption is that the scaling parameters r_1 and r_2 can be applied for the entire range of pressure heads under unsaturated conditions. Where the values of r_1 and r_2 equate to 1.0, the soil chemistry supports the maximum hydraulic conductivity.

The scaling parameter r_1 is based on the clay-swelling model of McNeal (1968). This describes the reduction of K_s in terms of the exchangeable sodium percentage (ESP) and electrolyte concentration using a montmorillonite interlayer swelling factor. The relationship between r_1 and the clay-swelling model (x) was calculated by McNeal (1968) and can be written as

$$r_1(\mathrm{SAR, EC}) = 1 - \frac{cx^n}{1+cx^n} \quad [3]$$

where c and n are empirical parameters for a given soil within a specified range of soil ESP, and x is the clay-swelling model calculated by McNeal (1968) based on the adjusted ESP and solution concentration. While beyond the scope of this study, it is noted here that the McNeal (1968) model was modified by Ezlit et al. (2013) to function on a soil-specific basis via a semiempirical disaggregation approach. Dang et al. (2018c) validated the specificity and the disaggregation model for field soils, while Bennett et al. (2019) demonstrated the magnitude of soil variability, even for the same soil orders. Therefore, in seeking to improve the soil-water dynamics of HYDRUS, it is prudent to utilize the semiempirical approach of Ezlit et al. (2013) as well as to seek to improve the incorporation of pH effects.

The r_2 scaling factor, for the effect of pH on the hydraulic conductivity, was calculated from the experimental data of Suarez et al. (1984) after first seeking to correct K_s reduction for the adverse effects of low electrolyte concentration and high exchangeable Na using r_1 (Eq. [3])—an attempt to provide the pH effect as independent of the SAR and EC combined effects. The following equation was developed by Suarez and Šimůnek (1997) and Šimůnek and Suarez (1997) based on the negative effects of the pH of the applied solution from the study of Suarez et al. (1984):

$$r_2(\mathrm{pH}) = \begin{cases} 1.0, & \text{for } \mathrm{pH} \le 6.83 \\ 3.46 - 0.36\mathrm{pH}, & \text{for } 6.83 < \mathrm{pH} < 9.3 \\ 0.1, & \text{for } \mathrm{pH} \ge 9.3 \end{cases} \quad [4]$$

The upper and lower pH limits are an assumption of no change in r_{Ks} or near-complete reduction for the specified pH ranges. We will refer to this model as the HYDRUS K–pH-dependent function. Consequently, the final hydraulic conductivity reduction due to the pH, SAR, and EC of the applied solution is calculated (Šimůnek and Suarez, 1997) as

$$\begin{aligned} K(h, \mathrm{pH, SAR, EC}) &= r(\mathrm{pH, SAR, EC}) K_s K_r(h) \\ &= r_1(\mathrm{SAR, EC}) r_2(\mathrm{pH}) K_s K_r(h) \end{aligned} \quad [5]$$

Equation [5] assumes that r_1 and r_2 have an equivalent weighted effect on the hydraulic reduction of the system, which allows the pH scaling factor to assert a large amount of control on the hydraulic system that may not necessarily be warranted.

Materials and Methods

Soil Selection and Initial Characterization

Nine soils were collected from the 0- to 30-cm depth of soils located in Queensland and New South Wales states, Australia (Table 1). The selection of these soils was based on their difference in initial pH and alkalinity as the primary selection factor. A secondary selection factor was the soil clay mineralogy and texture. The soils were air dried and crushed with sufficient energy to break down the aggregates to pass through a 2-mm sieve; care was taken to not apply energy greater than that required in order to maintain the physical bonds of the aggregates <2 mm. Using standard methods from Rayment and Lyons (2011), the electrical conductivity (Method 3A1), pH (Method 4A1), and soluble and exchangeable cations (Method 15A2) were measured. The alkalinity was determined using a Radiometer Analytical Titrator (TIM845, Titration Manager). Published methodologies were used to determine the soil particle size distribution (Gee and Bauder, 1986), clay mineralogy by X-ray diffraction (Jackson, 2005), and organic C (Walkley and Black, 1934). The soil characteristics are presented in Table 1.

Solution Preparation

The desired levels of pH, EC, and SAR of the experimental treatment solutions were obtained by mixing $NaHCO_3$, NaCl, and $MgCl_2 \cdot 6H_2O$ chemical compounds. Mixtures of Na and Mg salts rather than Na and Ca salts were used to prepare the solutions at each pH to prevent $CaCO_3$ precipitation at high pH and low SAR. The Mg concentration was calculated based on the soil-specific flocculation power from cation flocculation concentration experiments relative to Ca (Table 1) based on the modified method of Rengasamy and Oades (1977). The leaching solutions, SAR 20 and 40, were prepared at total electrolyte concentrations of 8, 15, 25, 50, and 100 $\mathrm{mmol_c\ L^{-1}}$ for SAR 20 and 8, 15, 25, 50, 100, 250, and 500 $\mathrm{mmol_c\ L^{-1}}$ for SAR 40 solutions. Both the SAR 20 and 40 solutions were then prepared at a equilibrated pH values of 6, 7, 8, and 9 according to the methodology of Suarez et al. (1984). The effective SAR ($\mathrm{SAR_{eff}}$) values were calculated based on the effective flocculation power of Mg:

$$\mathrm{SAR_{eff}} = \frac{\mathrm{Na}}{\sqrt{X\mathrm{Mg}/2}} \quad [6]$$

where X is the effective flocculation power of Mg exhibited for each soil (Table 1), and Na and Mg are concentrations (in $\mathrm{mmol_c\ L^{-1}}$).

The desired pH was achieved by adjusting the HCO_3^-/Cl^- ratio and CO_2 partial pressure (P_{CO2}) to ±0.05 units of the desired pH; the pH 9 and 6 solutions were the same except that the pH 9 solutions were equilibrated at atmospheric CO_2 ($P_{CO2} \approx 35$ Pa) and the pH 6 solution at $P_{CO2} \approx 97$ kPa using CO_2 gas with 99.9% purity. This was consistent with the methodology of Suarez et al. (1984) to allow direct comparison with their results. This approach was used, rather than the addition of other alkali or acidic compounds, for pH adjustment to avoid a change in ionic composition and electrolyte concentration of solutions. The pH 6 solutions were achieved by continuously bubbling CO_2 gas into the 5.0-L solution container. The pH of the solution was measured in the solution container before degassing could occur.

Preparation for, and Measurement of, Saturated Hydraulic Conductivity

An aliquot (300 g) of each soil was carefully packed into polyvinyl chloride columns (87.5-mm inner diameter)—mesh

Table 1. Physical and chemical properties of the selected soils (0–30-cm depth).

	Soil								
Property†	1	2	3	4	5	6	7	8	9
pH (1:5)	8.9	8.8	8.3	7.3	7.4	7.1	4.5	5.3	5.2
EC (1:5), dS m^{-1}	0.34	0.30	0.33	0.19	0.09	0.05	0.08	0.05	0.02
Total alkalinity, mg L^{-1}	207.2	157.1	164.3	75.0	89.3	55.0	0.0	15.7	7.0
SAR, $(mmol_c\ L^{-1})^{-0.5}$	1.9	4.3	6.0	3.1	0.2	0.1	0.9	1.9	1.8
CROSS $(mmol_c\ L^{-1})^{-0.5}$	2.5	4.6	6.7	3.5	0.3	0.5	1.2	2.5	2.0
ESP, %	3.0	11.68	9.9	0.2	0.4	0.6	3.2	7.7	8.2
EDP, %	4.4	12.5	11	1.6	2	2.3	5.2	10	9.2
CEC, $mmol_c\ kg^{-1}$	139	154	306	647	469	76	20	18	58
Organic C, mg kg^{-1}	1.1	1.6	0.6	1.3	1.6	1.6	1.5	1.6	1.3
Cl^-, mg kg^{-1}	174.0	60.0	8.0	120.0	30.0	20.0	33.0	10.0	10.0
NO_3–N, mg L^{-1}	18.0	60.0	1200.0	17.0	0.1	0.7	1.0	0.6	0.1
CFC of (Mg)	0.63	0.71	0.73	0.73	0.58	0.49	0.62	0.71	0.66
Clay, %	28.8	33.8	46.3	62.3	30.3	12.5	15.0	10.0	9.5
Silt, %	12.8	16.3	6.3	15.8	13.8	5.0	22.5	10.0	4.8
Sand, %	58.5	50.0	47.5	21.9	56.0	82.5	62.5	80.0	85.8
Taxonomic class									
Australian	Brown Dermosol	Red Dermosol	Gray Vertosol	Black Vertosol	Brown Vertosol	Red Kandosol	Gray Kurosol	Yellow Chromosol	Gray Chromosol
USDA	Inceptisol	Inceptisol	Vertisol	Vertisol	Vertisol	Inceptisol	Ultisol	Alfisol	Alfisol
Location in Australia	28°58′29″ S, 150°26′38″ E Wariven, NSW	28°54′50.48″ S, 150°16′18.6″ E Eldorado, NSW	27°49′50″ S, 150°9′13.9″ E Moonie, QLD	27°13′48″ S, 151°19′12″ E Dalby, QLD	27°48′32.8″ S, 151°54′22.2″ E Greenmount, QLD	27°58′8.4″ S, 148°22′51.6″ E St. George, QLD	25°21′36″ S, 152°44′40.44″ E Maryborough, QLD	27°35′44.9″ S, 152°18′20.1″ E Gatton, QLD	26°51′19.3″ S, 152°59′23.46″ E Beerwah, QLD

† EC, electrolyte concentration; SAR, sodium adsorption ratio; CROSS, cation ratio of soil structural stability; ESP, exchangeable sodium percentage; EDP, exchangeable dispersive percentage; CEC, cation exchange capacity; CFC of (Mg), the equivalent effectiveness of the flocculation power of Mg relative to Ca.

bottoms and a fast filter paper were used to allow drainage—to attain the mean bulk density (1.4 g cm^{-3}) for the nine soils. In a disturbed soil column, the bulk density is somewhat arbitrary, hence the mean value was considered an appropriate selection. The soil columns were initially saturated with the appropriate solution by capillary tension from the bottom of the core. Subsequently, the same solution was applied to the top of the column to measure the hydraulic conductivity at a constant hydraulic head of 2.0 cm, in accordance with Klute (1965). Leaching commenced with the most concentrated solution of the desired pH and SAR (Fig. 1 and 2). When the K_s of the soil columns and pH of the effluent had stabilized, the sequentially lower EC concentration solution of the same SAR and pH was applied. This process was continued until the culmination of the final solution in the sequence. The leachate solutions were collected from each column at time intervals to calculate K_s using Darcy's law. For the purposes of comparison, the K_s values were compared with the initial K_s values determined as the K_s occurring with the greatest electrolyte concentration (for SAR 20, the greatest EC was 100 $mmol_c\ L^{-1}$, and for SAR 40 it was 500 $mmol_c\ L^{-1}$). The K_s was calculated at sequential time intervals (t) using Darcy's law:

$$K_s = \frac{VL}{AHt} \quad [7]$$

where V is the volume of solution (cm^3), L is the length of the soil core (cm), A is the cross-sectional area of the soil column (cm^2), and H is the water head extending from the top of the ponded solution to the depth of the soil core (cm). Three replicates for each treatment and soil were used to determine K_s, creating a total of 216 soil cores for all soils used in this study.

The changes in hydraulic conductivity between treatments were represented as a relative hydraulic conductivity (r_{Ks}):

$$r_{Ks} = \frac{K_{s(i+n_j)}}{K_{si}} \quad [8]$$

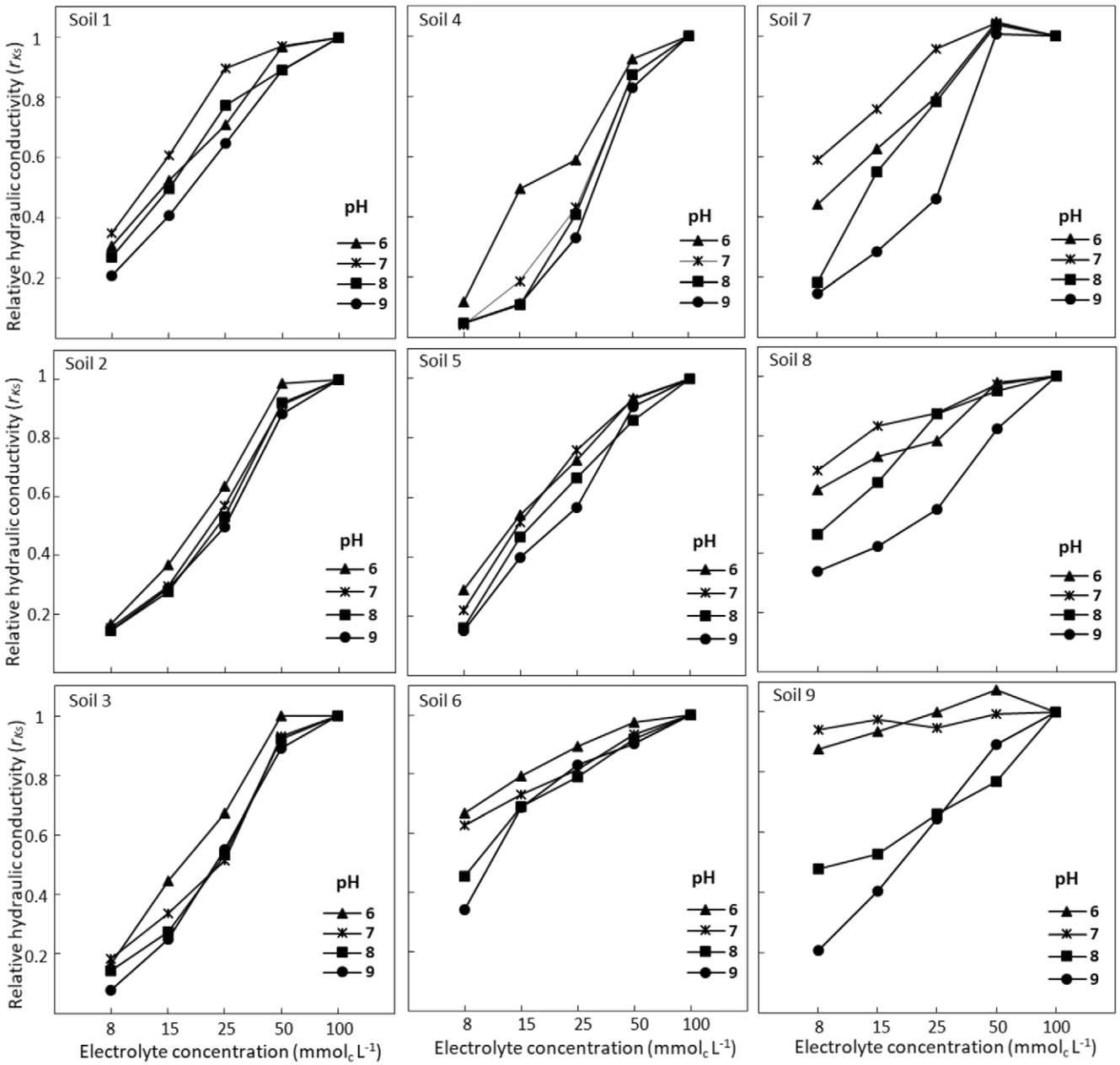

Fig. 1. Relative hydraulic conductivity (r_{Ks}) vs. electrolyte concentration for soils at a Na adsorption ratio of 20 and pH of 6, 7, 8, and 9.

where the initial K_s, denoted by i, was compared with the $i + n_j$ sequential K_s to provide a hydraulic conductivity reduction from the initial K_s, where n_j is the jth sequential solution in the sequence of n solutions.

Modification of the Hydraulic Reduction Scaling Factor for pH

Generalized Equation

An inverse empirical model for the prediction of the K_s reduction scaling factor, due to the adverse effects of irrigation water pH, was developed from the observed r_{Ks} data (Fig. 1 and 2). The r_2 scaling factor in HYDRUS proposed by Šimůnek and Suarez (1997) (Eq. [8]) was recalculated using the experimental r_{Ks} values from the study of Suarez et al. (1984). Subsequently, these r_{Ks} values were compared with the r_{Ks} values for the current experimental results observed at pH 6 [$r_{Ks(pH6)}$] for each EC value and SAR of 20 and 40. This provided an initial determination of the relative scaling factor (r_{SF}) for comparison purposes:

$$r_{SF} = \frac{rK_{s(i,n_i)}}{rK_{s(i)}} \quad [9]$$

where r_{SF} is the r_{Ks} reduction ratio compared with the r_{Ks} at pH 6 [$r_{Ks(i)}$], and n_j is the sequential solution pH in the solution sequence. After calculating the parameters from Eq. [9], a new r_2 pH scaling factor was then calculated using a linear regression analysis. Linear

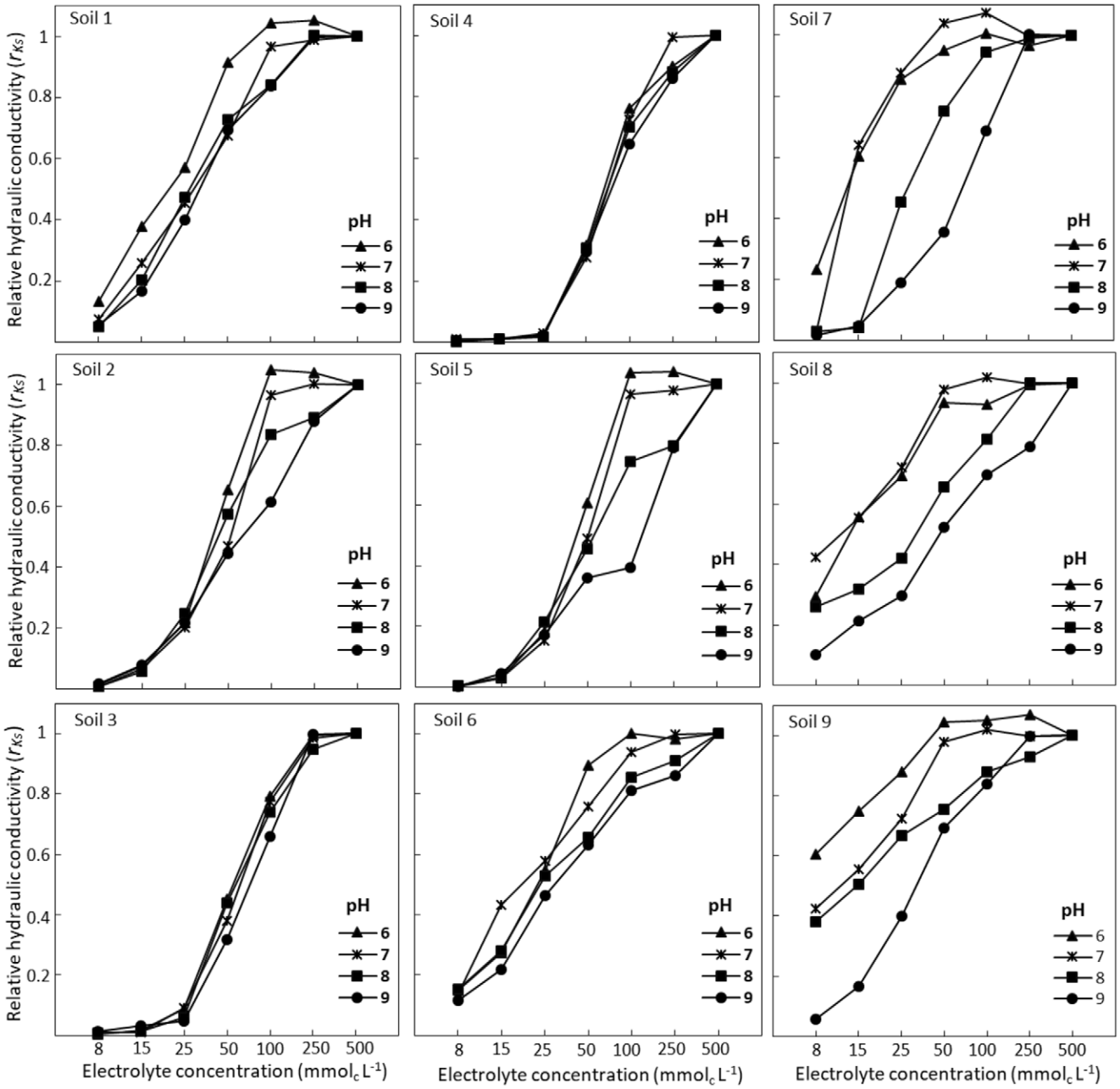

Fig. 2. Relative hydraulic conductivity (r_{Ks}) vs. electrolyte concentration for soils at a Na adsorption ratio of 40 and pH of 6, 7, 8, and 9.

regression was investigated in terms of the r_{Ks} for each pH and individual soil using the statistical program Minitab V.17 (Fig. 3). From these data, a generalized r_2 function was also formed using the same approach as Šimůnek and Suarez (1997), based on the results of r_{Ks} for the soils used in the study of Ali et al. (2019) and presented in (Fig. 1 and 2). This new generalized function is

$$r_2(pH) = \begin{cases} 1.0, & \text{for pH} < 7.2 \\ 2.242 - 0.172\text{pH}, & \text{for } 7.2 \le \text{pH} \le 9.5 \\ 0.60 & \text{for pH} > 9.5 \end{cases} \quad [10]$$

and the statistical parameters are presented in Table 2. We will refer to this model as the new generalized model.

Nonlinear Regression Using the Levenberg–Marquardt Method

After calculating the parameters for Eq. [9] by comparison of the K_s reduction data, a stepwise regression was then performed with solution pH, solution EC, soil pH and clay content included. As a result of this, soil pH was dropped from the model, with the remaining parameters significant and included in the model. Therefore, the solution pH, solution EC, and clay content were included in a nonlinear forecast model based on the observed training data using the statistical program Minitab V.17.

To find the coefficients of the nonlinear equation expressing the pH dependence of the soil K_s reduction, a

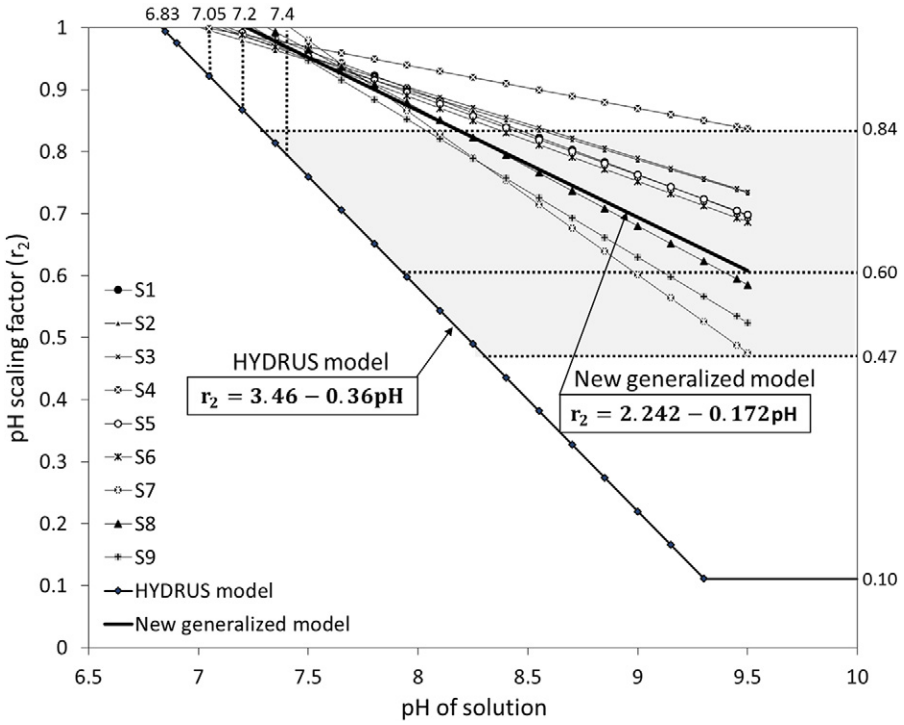

Fig. 3. The new generalized function and HYDRUS *K*–pH-dependent function to calculate the hydraulic conductivity scaling factor (r_2) due to the pH of the solution. The shaded region represents the range of variations for r_2 = 1.0 and r_2 = 0.1 for nine soils compared with the HYDRUS *K*–pH-reduction function; the central dotted line represents the r_1 and r_2 conditions for the generalized equation of these same nine soils.

Levenberg–Marquardt simulation optimization algorithm (Marquardt, 1963) was used, which served to iteratively solve an optimization problem of minimizing errors between the observed and computed values of the K_s reduction in relation to changes in the pH and EC of the solution and the clay content of the soils. This optimization was used to develop a prediction model for forward solutions. This approach works well in modeling situations because it specifically simulates the K_s reduction due to the pH of irrigation water and is amenable to continuous and adaptive solution EC, solution pH, and soil clay content, which is extremely desirable in governing K_s temporal and spatial dynamics (Benson and Trast, 1995; Frenkel et al., 1978). The r_2 scaling factor model, based on the Levenberg–Marquardt approach is

$$r_{LM} = \frac{1.25 - pH \times \ln(EC)}{21.72 - 7.42 \times pH + 28.8 \times \ln(EC) + 0.33 \times CC} \quad [11]$$

where r_{LM} is the predicted scaling factor for K_s reduction due to the pH of the percolating solution (pH), in tandem with the solution EC and clay content (CC); EC is measured in mmoles of charge per liter, while CC is a percentage of the total soil particle size analysis. The model parameters and associated statistics are presented in Table 3. We will refer to this model as the nonlinear model.

Evaluation of the Developed Models

The models were trained and evaluated against the measured K_s reduction data obtained for nine contrasting Australian soils at four different pH levels (Fig. 1 and 2). The observed r_{Ks} values were compared with the predicted r_{Ks} of the corresponding HYDRUS *K*–pH-dependent function, the new generalized model, and the nonlinear model developed by using the Levenberg–Marquardt optimization approach; r_{Ks} values were calculated using Eq. [8].

For the nonlinear model, the standard error, the root mean square error (RMSE), and the coefficient of determination (R^2) of both predicted and measured results were compared and slightly diverged from each other, showing a higher coefficient of determination (R^2 = 0.82 and *t*-test = 2.45) between the observed values and model-simulated r_{Ks} than the current HYDRUS and new generalized functions. Conversely, the HYDRUS *K*–pH-dependent model produced the highest standard error and RMSE and the lowest coefficient of determination (R^2 = 0.51 and *t*-test = 8.45) compared with the new generalized and nonlinear models for observed and simulated r_{Ks} values (Table 4).

The statistical analysis was also conducted among predicted r_{Ks} values for the HYDRUS *K*–pH-dependent function, the new generalized model, and the nonlinear function. A significant difference was observed (P < 0.001) for the new generalized model

Table 2. Statistical parameters for the HYDRUS *K*–pH-dependent function and the new generalized function calculated in this study using linear regression analysis, including the standard error of the regression (SE), Durbin–Watson statistic to detect the presence of autocorrelation (DWS), the root mean square error (RMSE), the coefficient of determination (R^2), adjusted coefficient of determination (R^2_{ADJ}), and predicted coefficient of determination (R^2_{PRED}); *F* value and *P* value are statistical tests to determine whether the term is associated with the response.

Equation	SE	DWS	RMSE	R^2	R^2_{ADJ}	R^2_{PRED}	*F* value	*P* value
HYDRUS *K*–pH-dependent function	0.53	2.14	0.78	0.36	0.33	0.22	14.3	0.001
New generalized function	0.17	2.14	0.2	0.56	0.55	0.52	59.2	<0.001

Table 3. Statistical characteristics pertaining to Eq. [11] from the nonlinear regression analysis using the Levenberg–Marquardt algorithm.

Parameter†	Eq. [11]			
	Summary			
Iterations	24			
Final SSE	5.64			
DFE	427			
MSE	0.013			
SE	0.11			
	Lack of fit			
df	211			
SS	2.759			
MS	0.013			
F value	0.98			
P value	0.56			
	Parameter estimates			
			95% Confidence interval	
Coefficient	Estimate	SE estimate	Lower limit	Upper limit
α_1	1.25	0.033	1.196	1.31
α_2	21.72	9.63	6.91	40.1
α_3	−7.42	1.58	−10.76	−4.95
α_4	28.76	2.96	24.0	34.54
α_5	0.33	0.056	0.23	0.45

† SSE, sum of squared errors; DFE, error degrees of freedom; MSE, mean square error; SE, standard error; df, degrees of freedom; SS, sum of squared deviations; *F* value and *P* value are statistical tests to determine whether the term is associated with the response that includes the predictors in the current model; α_1–α_5, coefficient estimates to describe the relationship between the response (r_{LM}) and the predictors (pH, electrical conductivity, and clay content).

Table 4. Summary statistical characteristics of the observed relative hydraulic conductivity (r_{Ks}) and predicted r_{Ks} using the HYDRUS *K*–pH-dependent model, the new generalized model, and the nonlinear model, which are shown in Fig. 4, using the analysis of variance and the *t*-test methods.

Statistic	HYDRUS *K*–pH-dependent function	New generalized function	Nonlinear function
SE	0.25	0.17	0.14
RMSE	0.32	0.18	0.16
R^2	0.51	0.77	0.81
R	0.72	0.88	0.90
t-test	8.45	2.86	2.45
F value	71.35	8.16	6.01
P value	<0.001	0.005	0.015

Table 5. Summary statistical characteristics of the observed relative hydraulic conductivity (r_{Ks}) from the study of Suarez et al. (1984) and predicted r_{Ks} using the HYDRUS *K*–pH-dependent model, the newly developed generalized equation, and the nonlinear equation, which are shown in Fig. 5, using the analysis of variance and the *t*-test methods.

Statistic	HYDRUS *K*–pH-dependent function	New generalized function	Nonlinear function
SE	0.30	0.24	0.20
RMSE	0.37	0.25	0.22
R^2	0.45	0.67	0.75
R	0.67	0.82	0.86
t-test	5.1	2.15	2.13
F value	25.77	4.5	4.4
P value	<0.001	0.034	0.035

and the nonlinear equation compared with the HYDRUS *K*–pH-dependent function, while no significant difference was detected ($P = 0.71$) between predicted r_{Ks} for the generalized and nonlinear equations. These statistics indicate that there was a better fit by the nonlinear model to the observed r_{Ks} data.

Validation of the New Scaling Factors

The two new regression models were validated against the experimentally observed r_{Ks} values of the California soils from the study of Suarez et al. (1984). Additionally, the HYDRUS *K*–pH-dependent model (Šimůnek and Suarez, 1997)—developed from the Suarez et al. (1984) data—was evaluated against the same California dataset to determine the magnitude of improvement that the new models provided. Statistical parameters for the observed vs. predicted values for each model are presented in Table 5.

Using the *t*-test and analysis of variance for the null hypothesis of no difference, the statistical tests showed that there was a significant difference between predicted and measured values of r_{Ks} using the HYDRUS *K*–pH-dependent model (*t*-test = 5.1, $P < 0.001$, $R^2 = 0.45$). A comparison was also made between the newly proposed generalized and nonlinear models and the observed r_{Ks} values of Suarez et al. (1984), providing *t*-test = 2.15, $P < 0.034$, $R^2 = 0.67$ and *t*-test = 2.13, $P < 0.035$, $R^2 = 0.75$, respectively. The tests indicated that there was a higher correlation between predicted and observed r_{Ks} values for these models than the HYDRUS *K*–pH-dependent function at the 0.05 probability level (Table 5). The statistics also showed a significant difference ($P < 0.001$) for the proposed generalized and nonlinear equations for the data from the Suarez et al. (1984) soils compared with the HYDRUS *K*–pH-dependent model; no significant difference was detected ($P = 0.93$) between the predicted r_{Ks} values of the generalized and nonlinear models.

Figures 4 and 5 indicate that the r_{Ks} data points are consistently better predicted using the new nonlinear equation, although the new generalized linear equation performs reasonably well in comparison. Interestingly, the HYDRUS *K*–pH-dependent model does not perform well on the data from which it was created. We propose that the better performance of the nonlinear equation suggests that soil-specific attributes of soils will be important in explaining the reduction in hydraulic dynamics. This result is not surprising, given the literature indicating that soil

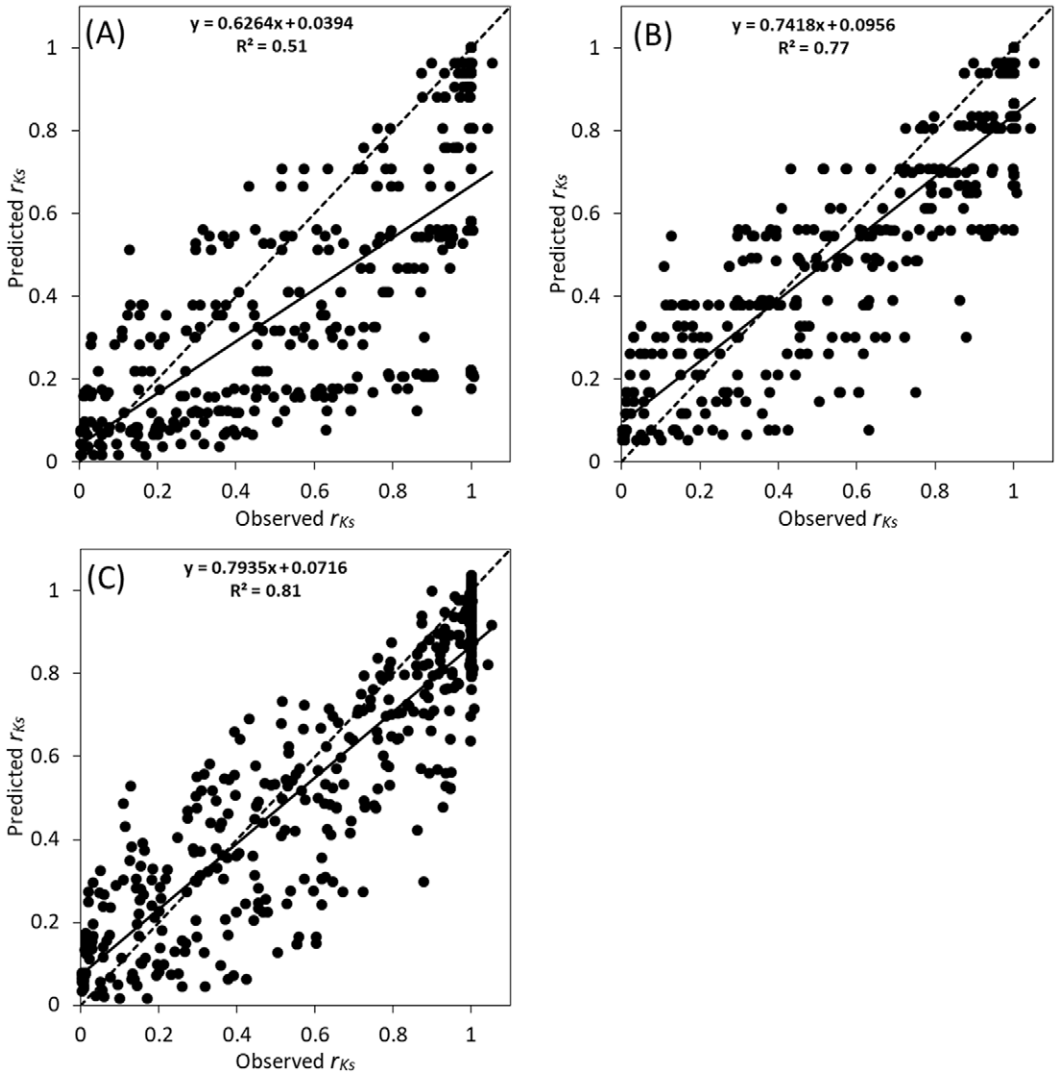

Fig. 4. The relation between the observed relative hydraulic conductivity (r_{Ks}) and r_{Ks} predicted using (A) the HYDRUS K–pH-dependent model, (B) the new generalized model, and (C) the nonlinear function (Levenberg–Marquardt algorithm). The diagonal dotted line is the 1:1 line, and the solid line is the regression fit for the observed data.

hydraulic reduction is soil specific (Bennett et al., 2019; Marchuk and Rengasamy, 2011), but it does reinforce the need to update such parameters within soil-water models.

Observed vs. Predicted Reduction in Hydraulic Conductivity

The statistical analysis showed the accuracy of the predicted r_{Ks} for each model for each dataset (Tables 4 and 5). For r_2 optimization, the new generalized and nonlinear models demonstrated better performance, as indicated by their lower RMSE and t-test values and higher coefficients of determination for the Australian and California soils. For both datasets, when the nonlinear model was used, the predicted outcomes were generally in closer agreement with the observations of r_{Ks} than the other two models.

Naturally, the observed r_{Ks} values are dependent on the EC, SAR, and pH of the solution, as well as the soil clay content and mineralogy (Bennett et al., 2019; McNeal and Coleman, 1966; Suarez et al., 1984). The relatively high accuracy and performance of the nonlinear model was mainly due to its capability of predicting pH effects more specifically by considering electrolyte concentration and clay content. The r_2 scaling factor for the nonlinear model (r_{2LM}) is mainly controlled by the pH and EC of the solution and the clay content of the soil, as shown by

$$K_{LM}(h, \text{pH, SAR, EC, CC}) = r_{LM}(\text{pH, SAR, EC, CC}) K_s K_r(h) \quad [12]$$

Comparatively, the r_2 scaling factor for the generalized models is simply based on the pH of the solution (Eq. [2]). Accordingly, the predicted r_{Ks} values were calculated using Eq. [5] and Eq. [13] to calculate the r_{Ks} of the generalized models and nonlinear model, respectively:

$$r_{LM}(\text{pH, SAR, EC, CC}) = r_1(\text{SAR,EC}) r_{2LM}(\text{pH,EC,CC}) \quad [13]$$

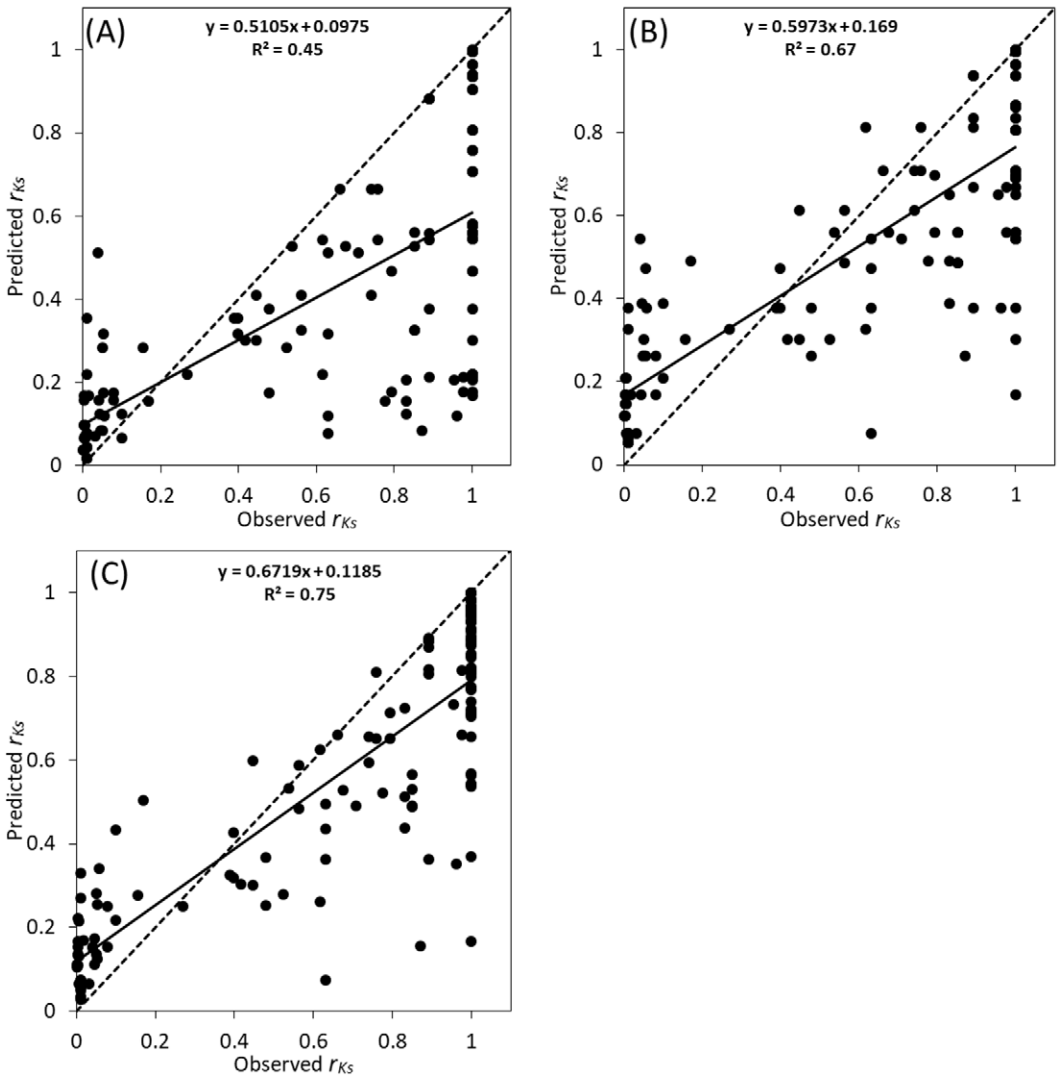

Fig. 5. The relation between the observed relative hydraulic conductivity (r_{Ks}) from the study of Suarez et al. (1984) and predicted r_{Ks} using (A) the HYDRUS K–pH-dependent model, (B) the new generalized model, and (C) the nonlinear model (Levenberg–Marquardt algorithm). The diagonal dotted line is the 1:1 line, and the solid line is the regression fit for the observed data.

where K_{LM} is the hydraulic conductivity based on the Levenberg–Marquardt nonlinear model (r_{2LM}; Eq. [11]), r_{LM} is the saturated hydraulic conductivity reduction as a result of adverse effects of EC, SAR, and pH (using the nonlinear function), and CC is the clay content (%).

Another limitation of the predicted hydraulic conductivity is that the final r_{Ks} is also dependent on the degradative effects of EC and SAR (r_1; Eq. [3]). The r_1 scaling factor has been generalized and determined empirically and its parameter values developed using only a narrow range of soils. In that matter, the use of generalized parameters would increase errors related to the uncertainty in the weighted scaling factors and result in reducing the accuracy of r_{Ks} prediction. The extent of uncertainty of the pH scaling factor (r_{2LM}) is somewhat reduced by including EC and clay content in the calculation of the scaling factor for the hydraulic dynamic reduction (Eq. [13]). This is a clear indication of the improvement of r_{Ks} prediction using the nonlinear function, although it could be further improved by combining r_1 and r_2 in a single nonlinear equation.

Discussion

Improvement of HYDRUS

The literature demonstrates that the HYDRUS models have been effectively applied to laboratory and field experiments (Ramos et al., 2011, 2012; Rasouli et al., 2013) using soil hydraulic conductivity and solute transport model parameters. Šimůnek et al. (2012) argued that the HYDRUS codes are physically based models and may require little or no calibration when all required input parameters are experimentally determined. However, in terms of hydraulic conductivity dynamic decline, there is no physical parameter that can be measured, and the functions describing reduction do not allow for soil-specific nuances. This is an important limitation of the current HYDRUS model family and

modules. Our work suggests that an updated generalized equation could be utilized, but it also further suggests that the inclusion of soil-specific attributes could provide a consistently better relation between observed and predicted results, which supports the use of and further development of the nonlinear function.

Using a broad range of soils, the principal goal of this current study was to evaluate the existing scaling factor (r_2) and its applicability, with the intent of improving on the existing HYDRUS reduction function to include soil-specific attributes. We have demonstrated that the generalized equation for the r_2 scaling factor of the HYDRUS model leads to a unique solution and can be updated using a broader range of soils. This allows the formation of soil-specific equations, in which the predicted r_{Ks} values are compared with observed r_{Ks} values for the 12 examined soils of Australia and California (Fig. 4 and 5). While the new generalized equation provided reasonable results over the existing linear HYDRUS equation, the nonlinear validated approach for K_s reduction will provide more confidence in the ability of the HYDRUS model to estimate dynamic K_s reduction. Soils are inherently heterogeneous in their properties and their resiliency to retain soil structure under conditions such as alkaline pH, low solution salinity, and adverse monovalent cation concentrations (dispersive potential varies). The Levenberg–Marquardt optimization allows the inclusion of multiple factors in a manner that provides a better fit to the complex nonlinear dynamics of soil hydraulic reduction.

Nonlinear Performance and Future Directions

The nonlinear inverse modeling included additional parameters, such as solution EC and soil clay content, which are critical governing factors in the management of the extent of K_s reduction (Agassi et al., 1981; Cook et al., 2006; Dang et al., 2018a, 2018c; Zhu et al., 2016). An increase in EC generates the osmotic pressure that compresses the diffuse double layer repulsive effect on the clay domains (Quirk, 2001), subsequently diminishing the contribution of pH and SAR on the diffuse double layer expansion (Sumner, 1993). The clay content is also an important factor in determining the extent of the hydraulic conductivity reduction and subsequently the resilience of the soil structure stability (Bennett et al., 2019). Concomitantly, the clay content of a soil has also been documented to affect the resilience of soil structure to the pH of the applied solution (Lieffering and McLay, 1996; Nyamangara et al., 2007). For lower clay content soils, the absolute decrease in K_s is greater than for clay soils, indicating the potential for negative effects of pH on K_s (Lieffering and McLay, 1996; Suarez et al., 1984). A similar trend was observed for K_s reduction in this study. Furthermore, in terms of the relative hydraulic reduction percentage, clay content will have an effect whereby highly sandy soils may require complete dispersion of the existing clay to cause a reduction percentage in K_s equivalent to the disaggregation properties in highly clay-dominant soils. This is considered as a function of the greater frequency of pores with smaller pore diameter and clay domain swelling without dispersion where sufficient clay exists. However, the agreement between the observed and predicted results for the nonlinear equation suggests that there is still a need for improvement in predictive capability.

Bennett et al. (2019) suggested that soil-specific hydraulic conductivity reduction functions require the consideration of clay properties, especially the quantification of clay mineral type, size, and surface charge, which reinforces the assertions of Quirk (2001). Additionally, and related to the clay specificity, the concept of ionicity affecting the net negative charge (Marchuk and Rengasamy, 2011) is also required to be incorporated into a soil-specific structural model (Bennett et al., 2019). Heterogeneous properties and the soil-specific behavior under the pH of applied solutions are known to affect the net negative charge (Chorom et al., 1994) and thereby provide a means of improving the prediction of hydraulic conductivity reduction.

It is also important to reflect on the fact that this study, and the study of Suarez et al. (1984)—the existing pH hydraulic reduction function within HYDRUS—examined repacked soil cores rather than undisturbed soils. This was to avoid heterogeneity factors that potentially mask the process effect of the mechanisms controlling hydraulic reduction. Importantly, we contend that the mechanisms controlling hydraulic conductivity reduction dynamics within a pore are consistent across all pore size ranges under both saturated and unsaturated conditions. This means that the scaling factor would apply uniformly to all pore sizes but that the absolute differences in hydraulic conductivity would depend on the pore size, inferring that the results in this study are applicable to both saturated and unsaturated conditions. However, the effect of pH on the hydraulic dynamics in an unsaturated soil was outside the scope of the current study and would be prudent to validate in future work.

Furthermore, there is merit in moving away from a scaling factor model that seeks to separate the cation and pH effects. Even with the improvement of the nonlinear model by including EC, it still fails to include the effects of cations on the dispersive, and thus hydraulic conductivity reductive, effects of SAR. The current dataset is insufficient to achieve this, with only two SAR levels; however, it does indicate that such a model can be achieved with reasonable confidence, given sufficient data. The level of confidence is an important topic to consider also. Bennett et al. (2019) demonstrated that a generalized equation for the soil-specific threshold electrolyte concentration (C_{TH}) varied by approximately $\pm$7.5 SAR units within one standard deviation, concluding that this level of variation within a generalized equation was not reliable and was environmentally unsound. However, the current scaling factor within HYDRUS is worse. The Ezlit et al. (2013) disaggregation model, which the Bennett et al. (2019) work is based on, was an improvement on the HYDRUS EC and SAR based reduction model (i.e., McNeal, 1968). On this basis, the first step would be to improve the current nonlinear approach to include the SAR effects within it and then incorporate this into HYDRUS, with a level of confidence surrounding the output for the user. Simultaneously, there is a requirement to improve the predictive capability from a fundamental point of view.

Soil Initial pH and Hydraulic Conductivity Reduction

The soil initial pH was dropped from the stepwise regression process, which led us to not include it within our models. This may suggest that the initial soil pH is not important in predicting the hydraulic conductivity decline. However, we caution that this assumption is on the basis of the study of Ali et al. (2019), who demonstrated that the initial soil pH and the clay content were both important in controlling the extent of the hydraulic conductivity reduction. The same nine soils were used in this work. It was observed by Ali et al. (2019) that while there was a significant reduction in soil structural characteristics for alkaline soils as pH increased, the concomitant extent of the K_s reduction was not significant, although it consistently decreased as pH increased. That is, the size of the reduction effect appeared to be controlled by the initial soil pH. The contrasting situation for an acidic initial soil pH interacted with lower clay content and, as this current work shows, outweighed in terms of the effect of clay content. For this reason, and the fact that the updated models were still developed on only 12 soils, it would be prudent to extend these studies to a broader range of soils that have varying pH and varying clay content within each pH subclass. As far as we are aware, combining the nine Australian soils and three California soils constitutes the most comprehensive dataset to determine the pH effect on soil hydraulic conductivity, which clearly identifies the requirement to increase the dataset such that the soil specificity is better captured within the nonlinear coefficients. This should further improve the nonlinear approach.

Conclusion

This research identified the limitation of the HYDRUS scaling factor (r_2) model and developed and validated two new models to optimize saturated hydraulic conductivity prediction. The proposed models were produced using a similar approach as in the HYDRUS model, with a nonlinear regression method further implemented. The nonlinear equation developed using the Levenberg–Marquardt algorithm considers the pH and EC of the solution, as well as the soil clay content, which is an important improvement toward soil-specific pedotransfer functions that may be incorporated into HYDRUS. The overall performance of the new models was significantly better than that of the existing linear HYDRUS hydraulic reduction scaling model. This was the case for both the current Australian dataset and for the California dataset on which the HYDRUS model was based.

Even though the prediction of the reduction in the hydraulic conductivity still has room for improvement in terms of the size of the dataset and soil types that control hydraulic conductivity reduction scaling factors and coefficients within the nonlinear model, the results significantly build on the existing circumstance. The nonlinear model, developed using the Levenberg–Marquardt approach to substitute the r_2 scaling factor in the HYDRUS program, provides a consistently more accurate estimate of the hydraulic conductivity than the current HYDRUS r_2 reduction model. Furthermore, the nonlinear equation is put forward as the basis for further improvement for the incorporation of identified soil properties suggested to govern soil structural dynamics.

Acknowledgments

Aram Ali wishes to acknowledge the University of Southern Queensland for provision of an international fee waiver and stipend scholarship in the pursuit of his doctoral qualification.

References

Agassi, M., I. Shainberg, and J. Morin. 1981. Effect of electrolyte concentration and soil sodicity on infiltration rate and crust formation. Soil Sci. Soc. Am. J. 45:848–851. doi:10.2136/sssaj1981.03615995004500050004x

Ali, A., J. Bennett, A. Biggs, and A. Marchuk. 2019. Effect of irrigation water pH on saturated hydraulic conductivity and electrokinetic properties of acidic, neutral and alkaline soils. Soil Sci. Soc. Am. J. 83:1671–1681. doi:10.2136/sssaj2019.04.0123

Assouline, S., and K. Narkis. 2011. Effects of long-term irrigation with treated wastewater on the hydraulic properties of a clayey soil. Water Resour. Res. 47:W08530. doi:10.1029/2011WR010498

Bell, F. 1996. Lime stabilization of clay minerals and soils. Eng. Geol. 42:223–237. doi:10.1016/0013-7952(96)00028-2

Ben-Hur, M., G. Yolcu, H. Uysal, M. Lado, and A. Paz. 2009. Soil structure changes: Aggregate size and soil texture effects on hydraulic conductivity under different saline and sodic conditions. Soil Res. 47:688–696. doi:10.1071/SR09009

Bennett, J.M., A. Marchuk, S. Marchuk, and S. Raine. 2019. Towards predicting the soil-specific threshold electrolyte concentration of soil as a reduction in saturated hydraulic conductivity: The role of clay net negative charge. Geoderma 337:122–131. doi:10.1016/j.geoderma.2018.08.030

Bennett, J.M., and B. Warren. 2015. Role of livestock effluent suspended particulate in sealing effluent ponds. J. Environ. Manage. 154:102–109. doi:10.1016/j.jenvman.2015.02.032

Benson, C.H., and J.M. Trast. 1995. Hydraulic conductivity of thirteen compacted clays. Clays Clay Miner. 43:669–681. doi:10.1346/CCMN.1995.0430603

Bolan, N.S., J.K. Syers, M.A. Adey, and M.E. Sumner. 1996. Origin of the effect of pH on the saturated hydraulic conductivity of non-sodic soils. Commun. Soil Sci. Plant Anal. 27:2265–2278. doi:10.1080/00103629609369702

Campbell, E.E., and K. Paustian. 2015. Current developments in soil organic matter modeling and the expansion of model applications: A review. Environ. Res. Lett. 10:123004. doi:10.1088/1748-9326/10/12/123004

Chorom, M., P. Rengasamy, and R. Murray. 1994. Clay dispersion as influenced by pH and net particle charge of sodic soils. Soil Res. 32:1243–1252. doi:10.1071/SR9941243

Cook, F.J., N.S. Jayawardane, D.W. Rassam, E.W. Christen, J.W. Hornbuckle, R.J. Stirzaker, et al. 2006. The state of measuring, diagnosing, ameliorating and managing solute effects in irrigated systems. Tech. Rep. 04/06. Coop. Res. Ctr. for Irrig. Futures, Darling Heights, QLD, Australia.

Dang, A., J.M. Bennett, A. Marchuk, A. Biggs, and S. Raine. 2018a. Evaluating dispersive potential to identify the threshold electrolyte concentration in non-dispersive soils. Soil Res. 56:549–559. doi:10.1071/SR17304

Dang, A., J.M. Bennett, A. Marchuk, A. Biggs, and S.R. Raine. 2018b. Quantifying the aggregation–dispersion boundary condition in terms of saturated hydraulic conductivity reduction and the threshold electrolyte concentration. Agric. Water Manage. 203:172–178. doi:10.1016/j.agwat.2018.03.005

Dang, A., J.M. Bennett, A. Marchuk, S. Marchuk, A. Biggs, and S. Raine. 2018c. Validating laboratory assessment of threshold electrolyte concentration for fields irrigated with marginal quality saline-sodic water. Agric. Water Manage. 205:21–29. doi:10.1016/j.agwat.2018.04.037

Ezlit, Y., J.McL. Bennett, S. Raine, and R. Smith. 2013. Modification of the McNeal clay swelling model improves prediction of saturated hydraulic conductivity as a function of applied water quality. Soil Sci. Soc. Am. J. 77:2149–2156. doi:10.2136/sssaj2013.03.0097

Frenkel, H., J. Goertzen, and J. Rhoades. 1978. Effects of clay type and content, exchangeable sodium percentage, and electrolyte concentration on clay dispersion and soil hydraulic conductivity. Soil Sci. Soc. Am. J. 42:32–39. doi:10.2136/sssaj1978.03615995004200010008x

Gee, G., and J. Bauder. 1986. Particle-size analysis. In: A. Klute, editor, Methods of soil analysis. Part 1. Physical and mineralogical methods. 2nd ed. SSSA Book Ser. 5. SSSA and ASA, Madison, WI. p. 383–411. doi:10.2136/sssabookser5.1.2ed.c15

Goldberg, S., and R.A. Glaubig. 1987. Effect of saturating cation, pH, and aluminum and iron oxide on the flocculation of kaolinite and montmorillonite. Clays Clay Miner. 35:220–227. doi:10.1346/CCMN.1987.0350308

Jackson, M.L. 2005. Soil chemical analysis: Advanced course. 2nd rev. ed. Parallel Press, Univ. of Wisconsin-Madison Libraries, Madison.

Klute, A. 1965. Laboratory measurement of hydraulic conductivity of saturated soil. In: C.A. Black et al., editors, Methods of soil analysis. Part 1. Physical and mineralogical properties. Agron. Monogr. 9. SSSA and ASA, Madison, WI. p. 210–221. doi:10.2134/agronmonogr9.1.c13

Lieffering, R.E., and C.D.A. McLay. 1996. The effect of strong hydroxide solutions on the stability of aggregates and hydraulic conductivity of soil. Eur. J. Soil Sci. 47:43–50. doi:10.1111/j.1365-2389.1996.tb01370.x

Marchuk, A., and P. Rengasamy. 2011. Clay behaviour in suspension is related to the ionicity of clay–cation bonds. Appl. Clay Sci. 53:754–759. doi:10.1016/j.clay.2011.05.019

Marchuk, A., and P. Rengasamy. 2012. Threshold electrolyte concentration and dispersive potential in relation to CROSS in dispersive soils. Soil Res. 50:473–481. doi:10.1071/SR12135

Marquardt, D.W. 1963. An algorithm for least-squares estimation of nonlinear parameters. J. Soc. Ind. Appl. Math. 11:431–441. doi:10.1137/0111030

McNeal, B. 1968. Prediction of the effect of mixed-salt solutions on soil hydraulic conductivity. Soil Sci. Soc. Am. J. 32:190–193. doi:10.2136/sssaj1968.03615995003200020013x

McNeal, B., and N. Coleman. 1966. Effect of solution composition on soil hydraulic conductivity. Soil Sci. Soc. Am. J. 30:308–312. doi:10.2136/sssaj1966.03615995003000030007x

Menezes, H., B. Almeida, C. Almeida, J. Bennett, E. Silva, and M. Freire. 2014. Use of threshold electrolyte concentration analysis to determine salinity and sodicity limit of irrigation water. Rev. Bras. Eng. Agric. Ambient. 18:53–58. doi:10.1590/1807-1929/agriambi.v18nsupps53-s58

Miller, D.A., and R.A. White. 1998. A conterminous United States multilayer soil characteristics dataset for regional climate and hydrology modeling. Earth Interact. 2:1–26. doi:10.1175/1087-3562(1998)002<0001:ACUSMS>2.3.CO;2

Nyamangara, J., S. Munotengwa, P. Nyamugafata, and G. Nyamadzawo. 2007. The effect of hydroxide solutions on the structural stability and saturated hydraulic conductivity of four tropical soils. S. Afr. J. Plant Soil 24:1–7. doi:10.1080/02571862.2007.10634773

Oades, J.M. 1984. Soil organic matter and structural stability: Mechanisms and implications for management. Plant Soil 76:319–337. doi:10.1007/BF02205590

Quirk, J. 2001. The significance of the threshold and turbidity concentrations in relation to sodicity and microstructure. Soil Res. 39:1185–1217. doi:10.1071/SR00050

Quirk, J., and R. Schofield. 1955. The effect of electrolyte concentration on soil permeability. J. Soil Sci. 6:163–178. doi:10.1111/j.1365-2389.1955.tb00841.x

Ramos, T.B., J. Šimůnek, M.C. Gonçalves, J.C. Martins, A. Prazeres, N.L. Castanheira, and L.S. Pereira. 2011. Field evaluation of a multicomponent solute transport model in soils irrigated with saline waters. J. Hydrol. 407:129–144. doi:10.1016/j.jhydrol.2011.07.016

Ramos, T.B., J. Šimůnek, M.C. Gonçalves, J.C. Martins, A. Prazeres, and L.S. Pereira. 2012. Two-dimensional modeling of water and nitrogen fate from sweet sorghum irrigated with fresh and blended saline waters. Agric. Water Manage. 111:87–104. doi:10.1016/j.agwat.2012.05.007

Rasouli, F., A.K. Pouya, and J. Šimůnek. 2013. Modeling the effects of saline water use in wheat-cultivated lands using the UNSATCHEM model. Irrig. Sci. 31:1009–1024. doi:10.1007/s00271-012-0383-8

Rayment, G.E. and D.J. Lyons. 2011. Soil chemical methods: Australasia. CSIRO Publ., Collingwood, VIC, Australia.

Rengasamy, P., and J. Oades. 1977. Interaction of monomeric and polymeric species of metal ions with clay surfaces: I. Adsorption of iron(III) species. Soil Res. 15:221–233. doi:10.1071/SR9770221

Rengasamy, P., and K. Olsson. 1991. Sodicity and soil structure. Soil Res. 29:935–952. doi:10.1071/SR9910935

Shainberg, I., and J. Letey. 1984. Response of soils to sodic and saline conditions. Calif. Agric. 52:1–57.

Šimůnek, J., M. Šejna, H. Saito, M. Sakai, and M.Th. van Genuchten. 2013. The HYDRUS-1D software package for simulating the movement of water, heat, and multiple solutes in variably saturated media, Version 4.17. HYDRUS Software Ser. 3. Dep. of Environmental Sciences, Univ. of California, Riverside.

Šimůnek, J., and D.L. Suarez. 1997. Sodic soil reclamation using multicomponent transport modeling. J. Irrig. Drain. Eng. 123:367–376. doi:10.1061/(ASCE)0733-9437(1997)123:5(367)

Šimůnek, J., M.Th. van Genuchten, and M. Šejna. 2012. HYDRUS: Model use, calibration, and validation. Trans. ASABE 55:1263–1276. doi:10.13031/2013.42239

Šimůnek, J., M.Th. van Genuchten, and M. Šejna. 2016. Recent developments and applications of the HYDRUS computer software packages. Vadose Zone J. 15(7). doi:10.2136/vzj2016.04.0033

Smith, W.N., W.D. Reynolds, R. de Jong, R.S. Clemente, and E. Topp. 1995. Water flow through intact soil columns: Measurement and simulation using LEACHM. J. Environ. Qual. 24:874–881. doi:10.2134/jeq1995.00472425002400050013x

Suarez, D., J. Rhoades, R. Lavado, and C. Grieve. 1984. Effect of pH on saturated hydraulic conductivity and soil dispersion. Soil Sci. Soc. Am. J. 48:50–55. doi:10.2136/sssaj1984.03615995004800010009x

Suarez, D.L., and A.G. Rubio. 2010. Season-long changes in infiltration rates associated with irrigation water sodicity and pH. In: R. Gilkes and N. Prakongkep, editors, Soil Solutions for a Changing World: Proceedings of the 19th World Congress of Soil Science, Brisbane, Australia. 1–6 Aug. 2010. Vol. WG 3. Int. Union Soil Sci. p. 54–56.

Suarez, D.L., and J. Šimůnek. 1997. UNSATCHEM: Unsaturated water and solute transport model with equilibrium and kinetic chemistry. Soil Sci. Soc. Am. J. 61:1633–1646. doi:10.2136/sssaj1997.03615995006100060014x

Sumner, M.E. 1993. Sodic soils: New perspectives. Soil Res. 31:683–750. doi:10.1071/SR9930683

Walkley, A., and I.A. Black. 1934. An examination of the Degtjareff method for determining soil organic matter, and a proposed modification of the chromic acid titration method. Soil Sci. 37:29–38. doi:10.1097/00010694-193401000-00003

Zhu, Y., A. Ali, A. Dang, A.P. Wandel, and J.M. Bennett. 2019. Re-examining the flocculating power of sodium, potassium, magnesium and calcium for a broad range of soils. Geoderma 352:422–428. doi:10.1016/j.geoderma.2019.05.041

Zhu, Y., A. Marchuk, and J.M. Bennett. 2016. Rapid method for assessment of soil structural stability by turbidimeter. Soil Sci. Soc. Am. J. 80:1629–1637. doi:10.2136/sssaj2016.07.0222